closo-Monocarbaboranes as Ligands for Transition Metals: Synthesis and Reactivity of *exo*-Diphosphineplatinum-*closo*-monocarbaborane Complexes; Structure of $[Pt\{Bu^t_2P(CH_2)_2PBu^t_2\}(closo\text{-}CB_{11}H_{12})][CB_{11}H_{12}]$†

Gaspar S. Mhinzi, Stephen A. Litster, Alan D. Redhouse and John L. Spencer*
Department of Chemistry and Applied Chemistry, University of Salford, Salford M5 4WT, UK

Protonation of the complexes $[PtR_2(L\text{–}L)]$ [R = Me, L–L = $(C_6H_{11})_2P(CH_2)_3P(C_6H_{11})_2$ **1a**; $Bu^t_2P(CH_2)_3PBu^t_2$, **1b**; $Bu^t_2P(CH_2)_2PBu^t_2$ **1c**; or $Bu^t_2PCH_2C_6H_4CH_2PBu^t_2$, **1d**; R = CH_2Bu^t, L–L = $(C_6H_{11})_2P(CH_2)_3P(C_6H_{11})_2$, **2a**; $Bu^t_2P(CH_2)_3PBu^t_2$, **2b**; or $Bu^t_2P(CH_2)_2PBu^t_2$, **2c**] with the monocarbaborane acid $HCB_{11}H_{12}$ in diethyl ether at 0 °C affords the *exo*-diphosphineplatinum-*closo*-monocarbaborane complexes $[Pt(L\text{–}L)(closo\text{-}CB_{11}H_{12})][CB_{11}H_{12}]$ [L–L = $(C_6H_{11})_2P(CH_2)_3P(C_6H_{11})_2$, **3a**, $Bu^t_2P(CH_2)_3PBu^t_2$, **3b**; $Bu^t_2P(CH_2)_2PBu^t_2$ **3c**; or $Bu^t_2PCH_2C_6H_4CH_2PBu^t_2$, **3d**] in which the co-ordinated *closo*-$CB_{11}H_{12}$ ligand is strongly bound to platinum *via* two *exo*-polyhedral three-centre two-electron (Pt ••• H ••• B) bridges. These complexes are fluxional in solution at room temperature. A single-crystal X-ray diffraction study of **3c** confirmed the bonding mode of the dodecaborane ligand. Complex **3c** crystallizes in the monoclinic space group $C2/c$, a = 16.199(4), b = 16.564(5), c = 14.896(3) Å, β = 93.64(2)° and Z = 4. The final discrepancy index was R = 0.043, R' = 0.050 for 2838 independent reflections. The geometry around the platinum centre is distorted square planar with μ-H-Pt 1.90(8), Pt-B 2.342(8) and B-μ-H 1.23(8) Å. In contrast when the solvent is changed from ether to tetrahydrofuran (thf), complex **1b** on protonation is converted into $[PtMe(thf)\{Bu^t_2P\text{-}P(CH_2)_3PBu^t_2\}][CB_{11}H_{12}]$ **5**. Complexes **3b**–**3d** react with acetonitrile to yield $[Pt(NCMe)_2(L\text{–}L)][CB_{11}H_{12}]_2$[L–L = $Bu^t_2P(CH_2)_3PBu^t_2$, **6b**; $Bu^t_2P(CH_2)_2PBu^t_2$, **6c**; or $Bu^t_2CH_2C_6H_4CH_2Bu^t_2$, **6d**]. Likewise **3b** reacts with pyridine affording $[Pt(NC_5H_5)_2\{Bu^t_2P(CH_2)_3PBu^t_2\}][CB_{11}H_{12}]_2$ **7**. However C_2H_4, CO and PPh_3 do not react readily with these complexes. The thf complex **5** reacts with deuteriated acetonitrile to form $[PtMe(NCCD_3)\{Bu^t_2P(CH_2)_3PBu^t_2\}][CB_{11}H_{12}]$ **8**. Spectroscopic data for the new complexes are presented and discussed.

Three-centre two-electron metal–hydrogen–boron bonds (M ••• H ••• B) in metallacarbaboranes may bridge two metal centres as in $[\{Ag(PPh_3)(C_2B_8H_{11})\}_2]$[1a] or $[MoW(\mu\text{-}CC_6H_4\text{-}Me\text{-}4)(CO)_3(\eta^5\text{-}C_9H_7)(\eta^5\text{-}7,8\text{-}C_2B_9H_9Me_2)]$,[1b] chelate as has been observed in some *exo-nido*-phosphinerhodacarbaboranes, for example $[Rh(PPh_3)_2(7\text{-}Me\text{-}8\text{-}Ph\text{-}7,8\text{-}C_2B_9H_{10})]$,[2] or one or two of the hydrogens of the carbaborane ligand can simply interact with the metal centre which may be positioned on the open face of the cage as in $[Co(\eta^5\text{-}C_5H_5)(nido\text{-}4\text{-}C_5H_5N\text{-}8,9\text{-}C_2B_8H_{10})]$.[3] Although transition-metal metallacarbaborane complexes in which the carbaborane ligand interacts with the metal centre *via* three-centre two-electron (M ••• H ••• B) bridges are well established, examples involving *closo*-carbaborane units are rare. This paper describes interesting new examples of complexes of this type.

In our continued investigation of the activation of C–H bonds by transition metals we were intrigued by the possibility of an α- or γ-C–H bond agostic interaction with the metal because it seems likely that these may be the intermediate states in α- or γ-elimination reactions. Following the synthesis of a range of complexes with β-agostic alkyl groups on a platinum centre and an examination of the ligand effects which might be responsible for the strength of the agostic interaction,[4,5] we wished to test whether the stereoelectronic properties which favour a β-agostic interaction will also favour α- or γ-agostic bonding.[6] It was therefore decided to extend the work by studying protonation reactions of complexes of the type $[PtR_2(L\text{–}L)]$ (R = Me or CH_2Bu^t, L–L = chelating diphosphine) with $HBF_4{\cdot}OMe_2$. Such protonations would leave a very reactive co-ordinately unsaturated (14-electron) platinum(II) centre, in which the electron deficiency might be relieved through a three-centre two-electron agostic interaction. However these reactions resulted in products which could not be completely characterized. This prompted us to explore alternative acids for the protonation reactions. The general chemical stability[7] and low nucleophilicity of the monocarba-*closo*-dodecaborane(12) anion ($CB_{11}H_{12}^-$) encouraged Scheidt and co-workers[8] to investigate its application as a non-co-ordinating counter ion for reactive co-ordinatively unsaturated metal cationic complexes. In fact this anion has been used successfully to stabilize the $[Fe(tpp)]^+$ (tpp = 5,10,15,20-tetraphenylporphyrinate) and $[PtH(PBu^t_3)_2]^+$ cations[9,10] as well as the complexes $[PtEt(L\text{–}L)]^+$ (L–L = chelating diphosphine)[5] which exhibits a β-C–H agostic interaction. Thus, the $CB_{11}H_{12}^-$ anion seemed to be a suitable alternative candidate as a non-co-ordinating anion for the cations which might be generated in the protonation of dimethyl or dineopentyl complexes. However the reaction of the *closo*-monocarbaborane acid ($HCB_{11}H_{12}$) with platinum(II) dimethyl or dineopentyl complexes in diethyl ether led to the elimination of both alkyl groups and the formation of *exo*- diphosphine-platinum-*closo*-monocarbaborane complexes exhibiting two three-centre two-electron (Pt ••• H ••• B) bridges as we describe in this paper.

---

† *Supplementary data available:* see Instructions for Authors, *J. Chem. Soc., Dalton Trans.*, 1991, Issue 1, pp. xviii–xxii.

Table 1 Elemental analyses[a] and IR and $^{31}P\text{-}\{^{1}H\}$ NMR[b] data

				Analysis (%)		$^{31}P\text{-}\{^{1}H\}$[b]	
Complex	Yield (%)	$\nu_{max}(BH)^{d}/cm^{-1}$	$\nu_{max}(Pt\cdots H\cdots B)^{d}/cm^{-1}$	C	H	δ	J(PtP)
1a $[PtMe_2(dcpp)]$	79			52.8 (52.6)	8.4 (8.5)	3.5	1866
1b $[PtMe_2(dbpp)]$	68			44.9 (45.2)	9.0 (8.7)	18.5	1826
1c $[PtMe_2(dbpe)]$	60			43.8 (44.2)	7.8 (8.5)	76.3	1806
1d $[PtMe_2(dbpx)]$	86			49.8 (50.4)	8.3 (8.1)	17.5	1850
2a $[Pt(CH_2Bu^t)_2(dcpp)]$	52			57.6 (57.4)	9.1 (9.4)	−4.4	1615
2b $[Pt(CH_2Bu^t)_2(dbpp)]$	60			52.1 (52.0)	10.0 (9.6)	13.6	1463
2c $[Pt(CH_2Bu^t)_2(dbpe)]$	55			51.2 (51.3)	9.7 (9.5)	67.1	1536
3a $[Pt(dcpp)(\textit{closo}\text{-}CB_{11}H_{12})][CB_{11}H_{12}]$	90	2552	2038	38.35 (37.95)	8.1 (8.1)	30.6	3327
3b $[Pt(dbpp)(\textit{closo}\text{-}CB_{11}H_{12})][CB_{11}H_{12}]$	88	2547	2029	30.8 (31.0)	8.5 (8.2)	51.0	3396
3c $[Pt(dbpe)(\textit{closo}\text{-}CB_{11}H_{12})][CB_{11}H_{12}]$	86	2541	2021	30.2 (30.0)	7.7 (8.1)	113.1	3526
3d $[Pt(dbpx)(\textit{closo}\text{-}CB_{11}H_{12})][CB_{11}H_{12}]$	94	2538	2029	35.8 (35.7)	8.0 (7.8)	49.2	3506
4 $[PtMe(CB_{11}H_{12})(dbpe)]$	*e*	2547		36.4 (35.8)	8.0 (8.3)	68.3 83.4	4583 1808
5 $[PtMe(thf)(dbpp)][CB_{11}H_{12}]\cdot C_4H_{10}O$	73	2539		41.7 (41.9)	9.3 (9.1)	26.1 28.1	4516 1827
6b $[Pt(NCMe)_2(dbpp)][CB_{11}H_{12}]_2$[f]	75	*e*		33.9 (33.5)	8.6 (8.1)	20.3	3442
6c $[Pt(NCMe)_2(dbpe)][CB_{11}H_{12}]_2$[f]	80	*e*		31.9 (32.7)	7.9 (8.0)	84.1	3566
6d $[Pt(NCMe)_2(dbpx)][CB_{11}H_{12}]_2$[f]	78	*e*		37.0 (37.6)	7.9 (7.8)	17.6	3548
7 $[Pt(NC_5H_5)_2(dbpp)][CB_{11}H_{12}]_2\cdot NC_5H_5$[f]	70	*e*		41.4 (41.1)	7.4 (7.8)	9.5	3143
8 $[PtMe(NCCD_3)(dbpp)][CB_{11}H_{12}]$	*e*	*e*		*e*	*e*	20.7 26.1	4248 1746
$[PtCl_2(dbpx)]$	37			43.6 (43.6)	6.6 (6.7)	10.5	3646

[a] Required values are given in parentheses. [b] Chemical shifts (δ) in ppm positive to high frequency of triphenyl phosphite (126.6) (external), coupling constants in Hz; measurements were made at room temperature. [c] All complexes were white except **3b**–**3d** and $[PtCl_2(dbpx)]$ which were pale yellow. [d] Nujol mulls. [e] Not determined. [f] Analysis: N, 3.3 (3.1), **6b**; 3.0 (3.2), **6c**; 2.7 (2.9), **6d**; 4.5 (4.0%), **7**

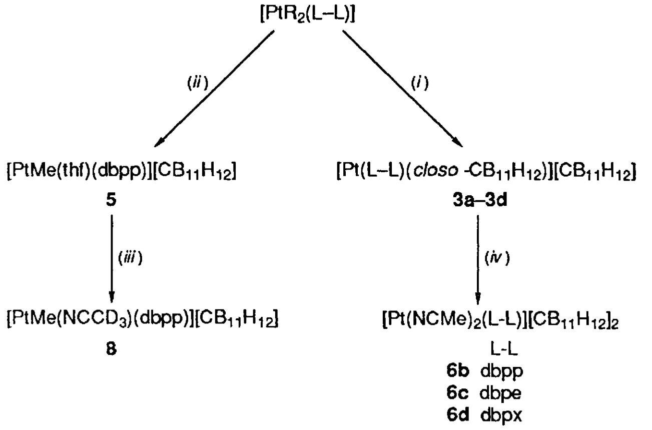

Scheme 1 R = Me, L–L = dcpp, **1a**; dbpp, **1b**; dbpe, **1c**; or dbpx, **1d**; R = CH_2Bu^t, L–L = dcpp, **2a**; dbpp, **2b**; or dbpe, **2c**. Only **1b** was used for reaction (*ii*). (*i*) $HCB_{11}H_{12}$ in diethyl ether at 0 °C; (*ii*) $HCB_{11}H_{12}$ in thf at 0 °C; (*iii*) CD_3CN; (*iv*) MeCN

Results and Discussion

Synthesis, Characterization, and Fluxional Behaviour of the exo-*Diphosphineplatinum*-closo-*monocarbaborane Complexes*.—Treatment of [PtR₂(cod)] (R = Me or CH_2Bu^t, cod = cycloocta-1,5-diene)[11,12] with diphosphines affords the white crystalline solids $[PtR_2(L\text{–}L)]$ [R = Me, L–L = $(C_6H_{11})_2P(CH_2)_3P(C_6H_{11})_2$ (dcpp), **1a**; or $Bu^t{}_2P(CH_2)_3PBu^t{}_2$ (dbpp), **1b**; R = CH_2Bu^t, L–L = dcpp, **2a**; dbpp, **2b**; or $Bu^t{}_2P(CH_2)_2PBu^t{}_2$ (dbpe), **2c**]. The complexes $[PtR_2(L\text{–}L)]$ [R = Me, L–L = dbpe, **1c**; or $Bu^t{}_2PCH_2C_6H_4CH_2PBu^t{}_2$ (dbpx), **1d**] were prepared by the reaction of the corresponding diphosphine with *cis*-$[PtCl_2(NCBu^t)_2]$ followed by conventional alkylation using methyllithium. The analytical and spectroscopic data for these complexes (summarized in Tables 1 and 2) are typical for complexes of the type $[PtR_2L_2]$ (R = Me or CH_2Bu^t; L = tertiary phosphine).[13,14] Reaction of **1a**–**1c** or **2a**–**2c** with the monocarbaborane acid $HCB_{11}H_{12}$ in a 1:1 mole ratio in diethyl ether at 0 °C affords a series of *exo*-diphosphineplatinum-*closo*-monocarbaborane complexes $[Pt(L\text{–}L)(\textit{closo}\text{-}CB_{11}H_{12})]^+$ (L–L = dcpp, **3a**; dbpp, **3b**; or dbpe, **3c**) (Scheme 1), the two methyl groups in **1a**–**1c** and the two neopentyl groups in **2a**–**2c** being replaced by the monocarba-*closo*-dodecaborane(12) anion. The complex cations crystallize with a second equivalent of $[CB_{11}H_{12}]^-$ as the counter ion. The characterization of these complexes is discussed in detail below. For **1c**, an ether-insoluble product which from spectroscopic data and elemental analysis may be formulated as $[PtMe(CB_{11}H_{12})(dbpe)]$ **4**, was also formed. Efforts to grow crystals suitable for X-ray diffraction for this complex have

Table 2 Proton,[a] $^{13}C-\{^1H\}$,[a] and $^{11}B-\{^1H\}$ NMR[b] data

Complex	$^1H(\delta)$[c]	$^{13}C-\{^1H\}$ (δ)
1a	0.23 [6 H, br t, $PtCH_3$, *J*(PtH) 66], 1.00–2.30 (50 H, br m, $PCH_2CH_2CH_2P$ and C_6H_{11})	2.7 (2 C, t, PCH_2), 25.1 (1 C, s, $PCH_2\mathit{C}H_2CH_2P$), 26.9–30.4 (br m, C_6H_{11}), 35.4 [4 C, br m, $P\mathit{C}(C_6H_{11})$]
1b	0.50 [6 H, tt, $PtCH_3$, *J*(PtH) 68, *J*(PH) 5.8], 1.29 [36 H, d, Bu^t, *J*(PH) 11], 1.77 (4 H, m, CH_2), 1.91 (2 H, m, CH_2)	2.2 [2 C, td, $PtCH_3$, *J*(PtC) 590, $J(PC)_{trans}$ 100, $J(PC)_{cis}$ 11], 21.9 (2 C, t, PCH_2), 25.0 (1 C, s, $PCH_2\mathit{C}H_2CH_2P$), 31.1 (12 C, s, Bu^t), 36.8 [4 C, s, $P\mathit{C}(CH_3)_3$]
1c	0.59 [6 H, tt, $PtCH_3$, *J*(PtH) 69, *J*(PH) 6], 1.24 [36 H, d, Bu^t, *J*(PH) 12], 1.67 (4 H, m, PCH_2)	0.7 [2 C, td, $PtCH_3$, $J(PC)_{trans}$ 97, $J(PC)_{cis}$ 8], 25.8 [2 C, t, PCH_2, $^1J(PC)$ 17], 30.5 (12 C, s, Bu^t), 36.1 [4 C, d, $P\mathit{C}(CH_3)_3$, *J*(PC) 16]
1d	0.50 [6 H, tt, $PtCH_3$, *J*(PtH) 69], 1.40 [36 H, d, Bu^t, *J*(PH) 11], 3.70 (4 H, br s, CH_2), 7.10, 7.30 (4 H, m, C_6H_4)	4.0 [2 C, td, $PtCH_3$, *J*(PtC) 590, $J(PC)_{trans}$ 99], 27.2 (2 C, s, PCH_2), 31.5 (12 C, s, Bu^t), 38.3 [4 C, t, $P\mathit{C}(CH_3)_3$], 125.8, 132.8, 138.1 (s, C_6H_4)
2a	1.10 [18 H, s, $CH_2C(C\mathit{H}_3)_3$], 1.20–1.90 (54 H, br m, $PCH_2CH_2CH_2P$ and C_6H_{11})	19.4 [2 C, t, PCH_2, *J*(PC) 12], 25.4 (1 C, s, $PCH_2\mathit{C}H_2CH_2P$), 25.7 [2 C, tdd, $PtCH_2$, *J*(PtC) 702, *J*(PC) 102], 27.1, 27.8, 29.6 (24 C, s, C_6H_{11}), 36.7 [6 C, t, $PtCH_2C(\mathit{C}H_3)_3$, *J*(PtC) 44]
2b	1.30 [36 H, d, Bu^t, *J*(PH) 10], 1.50 [18 H, s, $CH_2C(C\mathit{H}_3)_3$], 2.20 (4 H, m, PCH_2), 3.20 (2 H, m, $PCH_2C\mathit{H}_2$)	17.4 [2 C, td, $PtCH_2$, *J*(PtC) 741, *J*(PC) 94], 21.7 [2 C, s, PCH_2, *J*(PC) 10], 23.1 (1 C, s, $PCH_2\mathit{C}H_2CH_2P$), 30.5 (12 C, s, Bu^t), 36.8 [6 C, t, $PtCH_2C(\mathit{C}H_3)_3$, *J*(PtC) 45]
2c[d]	1.10 [18 H, s, $CH_2C(C\mathit{H}_3)_3$], 1.30 [36 H, d, Bu^t, *J*(PH) 9], 1.80 [4 H, br s, PCH_2 or $C\mathit{H}_2C(CH_3)_3$], 3.00 [4 H, br s, PCH_2 or $C\mathit{H}_2C(CH_3)_3$]	16.7 [2 C, td, $PtCH_2$, *J*(PtC) 720, *J*(PC) 104], 24.3 [2 C, t, PCH_2, *J*(PC) 16], 30.8 (12 C, s, Bu^t), 34.6 (2 C, s, $PtCH_2\mathit{C}$), 37.3 [6 C, t, $PtCH_2C(\mathit{C}H_3)_3$, *J*(PtC) 46]
3a[d]	−1.7 (2 H, br, Pt···H···B), 0.80–2.75 (50 H, br m, $PCH_2CH_2CH_2P$ and C_6H_{11})	15.8 [2 C, t, PCH_2, *J*(PC) 11], 22.5 (1 C, s, $PCH_2\mathit{C}H_2CH_2$), 25.4, 26.5, 29.0, 29.8 (20 C, s, C_6H_{11}), 39.1 [4 C, t, PC, *J*(PC) 17], 51.8 (1 C, s, $CB_{11}H_{12}^-$), 52.7 (1 C, s, $PtCB_{11}H_{12}$)
3b[e]	1.40 [36 H, d, Bu^t, *J*(PH) 16], 2.16 (4 H, m, PCH_2), 2.40 (2 H, br m, $PCH_2C\mathit{H}_2CH_2P$), 2.80 [1 H, br s, CH (cage)]	15.6 (2 C, br m, PCH_2), 18.6 (1 C, br s, $PCH_2\mathit{C}H_2CH_2$), 29.8 (12 C, br s, Bu^t), 39.9 [4 C, m, $P\mathit{C}(CH_3)_3$], 51.4 (1 C, br s, $CB_{11}H_{12}^-$), 52.9 (1 C, br s, $PtCB_{11}H_{12}$)
3c	1.57 [36 H, d, Bu^t, *J*(PH) 16], 2.25 [1 H, br s, $CH(CB_{11}H_{12}$–Pt)], 2.84 (4 H, m, PCH_2), 3.22 [1 H, br s, CH (cage)]	24.9 (2 C, m, PCH_2), 29.8 (12 C, br s, Bu^t), 39.7 [4 C, t, $P\mathit{C}(CH_3)_3$, *J*(PC) 14], 51.5 (1 C, s, $CB_{11}H_{12}^-$), 54.3 (1 C, br s, $PtCB_{11}H_{12}$)
3d[f]	−3.40 (2 H, br s, Pt···H···B), 1.57 [36 H, d, Bu^t, *J*(PH) 15], 2.23 [1 H, br s, CH (cage)], 3.24 [1 H, br s, CH (cage)], 4.50 [4 H, d, PCH_2, *J*(PH) 13], 7.44, 7.75 (4 H, m, C_6H_4)	26.8 (2 C, m, PCH_2), 31.7 (12 C, br s, Bu^t), 41.6 [4 C, d, $P\mathit{C}(CH_3)_3$, *J*(PC) 24], 51.5 (1 C, s, $CB_{11}H_{12}^-$), 52.6 (1 C, s, $PtCB_{11}H_{12}$)
4[d]	0.98 [3 H, td, $PtCH_3$, *J*(PtH) 45, *J*(PH) 7], 1.37 [36 H, d, Bu^t, *J*(PH) 13], 1.70 (2 H, m, PCH_2), 2.00 (2 H, m, PCH_2), 2.30 [1 H, br s, CH(cage)]	7.0 [1 C, td, $PtCH_3$, *J*(PtC) 429, *J*(PC) 87], 20.4 (1 C, m, PCH_2), 27.2 (1 C, m, PCH_2), 30.2 (6 C, s, Bu^t), 30.4 (6 C, s, Bu^t), 36.6 [2 C, d, $P\mathit{C}(CH_3)_3$, *J*(PC) 15], 38.0 [2 C, d, $P\mathit{C}(CH_3)$, *J*(PC) 30], 51.4 (br s, $CB_{11}H_{12}$)
5[e]	0.75 [3 H, td, $PtCH_3$, *J*(PtH) 42, *J*(PH) 7], 1.40 [36 H, dd, Bu^t, *J*(PH) 12], 1.83 (4 H, m, thf), 1.95 (4 H, br s, PCH_2), 2.07 (2 H, br s, $PCH_2C\mathit{H}_2CH_2P$), 3.70 (4 H, m, thf), 6.50 [1 H, br s, CH(cage)]	4.2 [1 C, td, $PtCH_3$, *J*(PtC) 459, *J*(PC) 83], 20.6 (2 C, m, PCH_2), 23.7 (1 C, m, $PCH_2\mathit{C}H_2CH_2P$], 26.2 (2 C, s, thf), 30.4 (6 C, s, Bu^t), 31.4 (6 C, s, Bu^t), 37.4 [2 C, d, $P\mathit{C}(CH_3)_3$, *J*(PC) 17], 38.8 (2 C, d, $P\mathit{C}(CH_3)_3$, *J*(PC) 32], 51.2 (1 C, s, $CB_{11}H_{12}^-$), 68.1 (2 C, s, thf)
6b[g]	1.41 [36 H, d, Bu^t, *J*(PH) 16], 1.52 (22 H, s, $CB_{11}H_{12}^-$), 1.97 (6 H, s, $NCC\mathit{H}_3$), 2.12 (4 H, m, PCH_2), 2.15 (2 H, br s, $PCH_2C\mathit{H}_2CH_2P$), 2.80 [2 H, br s, CH(cage)]	
6d[g]	1.46 [36 H, d, Bu^t, *J*(PH) 15], 1.90 (6 H, s, $NCC\mathit{H}_3$), 2.32 [2 H, br s, CH(cage)], 3.80 [4 H, d, PCH_2, *J*(PH) 11], 7.30, 7.47 (4 H, m, C_6H_4)	
7[h]	1.37 [36 H, d, Bu^t, *J*(PH) 14], 1.90–3.40 (br, $PCH_2CH_2CH_2P$ and $CB_{11}H_{12}^-$), 5.67, 7.20, 8.71 [s, β, γ, α, H of NC_5H_5]	18.7 [2 C, t, PCH_2 *J*(PC) 7], 21.5 (1 C, s, $PCH_2\mathit{C}H_2CH_2P$), 31.2 (12 C, s, Bu^t), 127.8 (2 C, m, C^2 of NC_5H_5, 142.2 (1 C, t, C^3 of NC_5H_5, 152.3 (2 C, br t, C^1 of NC_5H_5)
8[g]	0.78 [3 H, tdd, *J*(PH) 6, *J*(PtH) 43], 1.30 [36 H, dd, Bu^t, *J*(PH) 13], 1.90 (4 H, br m, PCH_2), 1.95 (2 H, br s, $PCH_2C\mathit{H}_2CH_2P$), 2.10 (6 H, s, $NCC\mathit{H}_3$), 2.30 [1 H, br s, CH(cage)]	19.9 (2 C, m, PCH_2), 23.8 (1 C, t, $PCH_2\mathit{C}H_2CH_2P$), 30.3 (6 C, s, Bu^t), 31.6 (6 C, s, Bu^t), 37.7 [2 C, d, PC *J*(PC) 17], 39.0 (2 C, d, PC)
$[PtCl_2(dbpx)]$	1.56 [36 H, d, Bu^t, *J*(PH) 13], 3.70 (4 H, br s, PCH_2), 7.20, 7.30 (4 H, m, C_6H_4)	30.2 [2 C, br t, PCH_2, *J*(PC) 11], 32.3 (12 C, s, Bu^t), 40.9 [4 C, br t, $P\mathit{C}(CH_3)_3$, *J*(PC) 25], 127.7, 133.2, 135.8 (6 C, s, C_6H_4)

[a] Chemical shifts (δ) in ppm positive to high frequency of $SiMe_4$, coupling constants in Hz, measurements at room temperature, solvent CD_2Cl_2 unless stated otherwise. [b] $^{11}B-\{^1H\}$ NMR; δ −7.5 (1 B, s), −13.7 (5 B, s), −16.4 (5 B, s), **3b**; −6.7 (1 B, s), −13.2 (5 B, s), −16.3 (5 B, s), **3c**; −6.8 (1 B, s), −13.3 (5 B, s), −16.4 (5 B, s), **5**. Chemical shifts are positive to high frequency of $BF_3 \cdot OEt_2$ (external). [c] Unless stated otherwise, chemical shifts for B–H groups occur as broad unresolved signals in the ranges 0–1.5. [d] In $CDCl_3$. [e] In C_4D_8O. [f] In $(CD_3)_2CO$. [g] In CD_3CN. [h] In NC_5D_5.

so far been unsuccessful. The exact structure of complex **4** is thus still unclear and is the subject of continuing investigation.

The reaction of **1d** with the monocarbaborane acid in a 1:1 mole ratio in diethyl ether resulted in products which could not be characterized. When a 1:2 mole ratio was used, however, the corresponding *exo*-diphosphineplatinum-*closo*-monocarbaborane complex $[Pt(dbpx)(\mathit{closo}\text{-}CB_{11}H_{12})][CB_{11}H_{12}]$ **3d** was formed in 94% yield. Similar reactions with **1a–1c** or **2a–2c** also afforded **3a–3c** respectively as the sole products. In contrast, when the solvent was changed from ether to tetrahydrofuran (thf) and the reactants were mixed either in a 1:1 or 1:2 mole ratio, complex **1b** was converted into $[PtMe(thf)(dbpp)][CB_{11}H_{12}]$ **5** in 73% yield.

The IR spectra (Nujol mull) of compounds **3a–3d** (Table 1) each show a strong broad peak characteristic of terminal B–H bonds[15] together with a medium peak (ν_{max} 2038, **3a**; 2029, **3b**; 2021, **3c**; 2029 cm^{-1}, **3d**) assigned to three-centre two-electron

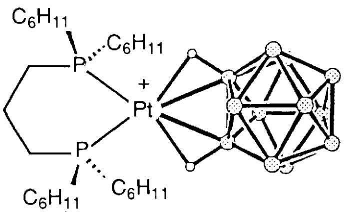

3a

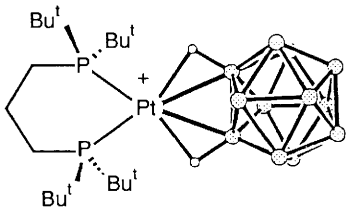

3b

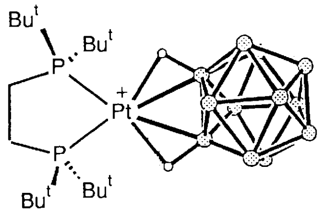

3c

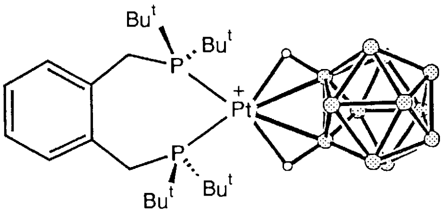

3d

bridges (Pt ··· H ··· B). The ^{1}H NMR spectra of **3b** and **3c** (Table 2) do not show any resonances assignable to (Pt ··· H ··· B) bridge bonds. However **3a** and **3d** display very broad resonances at δ −1.70 and −3.40 respectively corresponding to (Pt ··· H ··· B) bridge bonds.[16,17] These results suggest that for complexes **3a–3d** there probably exists a rapid dynamic process that serves to exchange the terminal B–H hydrogens with the (Pt ··· H ··· B) hydrogens as has been observed in some *exo-nido*-phosphinerhodacarbaboranes.[17] The ^{1}H NMR signals for the other terminal B–H protons for **3a–3d** are not resolved and appear as a broad signal at δ 0–1.5. Cooling **3b** to −40 °C resulted in the appearance of a broad signal at δ −3.3 corresponding to the (Pt ··· H ··· B) bridges and the signal for the Bu^t groups changed from a doublet to an overlapping pair of doublets with the appearance of a triplet. Although boron decoupling may be achieved by lowering the temperature,[18] further cooling to −66 °C had no effect on the broad signal for the bridging hydrogens and no Pt–H coupling could be observed. The signal for the Bu^t groups was split into two separate doublets at low temperature.

Consistent with the presence of two carbaborane cages are the ^{13}C-{^{1}H} NMR spectra of compounds **3a–3d** (Table 2) which show two broad peaks (δ 51.8, 52.7, **3a**; 51.4, 52.9, **3b**; 51.5, 54.3, **3c**; 51.5, 52.6, **3d**) corresponding to the carbon atoms of the counter ion and the co-ordinated cages respectively. The thf complex **5** shows one signal only (δ 51.2) assignable to the carbon atom of the counter ion. No resonances assignable to a methyl or a neopentyl group for **3a–3d** were observed. The absence of any Pt–C coupling in the resonances for the carbon atoms of the carbaborane cages ruled out any possibility of Pt–C bonding in the *exo*-diphosphineplatinum-*closo*-monocarbaborane complexes. The ^{31}P-{^{1}H} NMR spectra of **3a–3d** (Table 1) at *ca.* 20 °C each show a single signal with platinum-195 satellites, implying either real or time-averaged molecular symmetry. In order to explore further the behaviour of these *exo*-diphosphineplatinum-*closo*-monocarbaborane complexes the low-temperature ^{31}P-{^{1}H} NMR spectrum of **3b** was recorded. As expected at −80 °C the two different phosphorus environments could be detected on the NMR time-scale and the single signal is split into two sharp signals [δ 50.2, ^1J(PtP) = 3377, ^2J(PP) = 9; δ 51.7, ^1J(PtP) = 3420, ^2J(PP) = 9 Hz]. Presumably the asymmetry observed at low temperature arises as a result of the position of the cage carbon atom relative to the {Pt(L–L)} group. Rotation about the metal-cage axis at higher temperatures would lead to the observed equivalence of the phosphorus environments.

The ^{11}B-{^{1}H} NMR spectra of compounds **3b** and **3c** (Table 2) at *ca.* 20 °C each show three sharp signals assignable to the carbaborane counter ion only.[19] At −96 °C however, the spectrum of **3b** shows an additional sharp signal at δ −22.1 which may be assigned to the unique boron atom directly opposite the carbon atom of the co-ordinated carbaborane cage, together with two very broad unresolved peaks at δ *ca.* −43.4 and *ca.* 40.0. The latter are of no value in the assignment of the different boron atoms in the co-ordinated cage. Thus it appears that in solution the *exo*-diphosphine-platinum-*closo*-monocarbaborane complexes are fluxional to as low as −96 °C and it has so far proved impossible to determine which boron atoms are attached to platinum. The two broad signals in the low-temperature ^{11}B-{^{1}H} NMR spectrum of **3b** (δ *ca.* −43.4, 40.0), however, suggest that in solution the {Pt(L–L)} fragment may move from one pair of boron atoms to another, resulting in the averaged broad resonances which are observed. It is worthwhile noting also that the ^{13}C-{^{1}H} NMR signal for the carbon atom of the co-ordinated cage in **3a–3d** is not severely shifted from that of the counter ion, implying that whatever the fluxional process the proximity effect of the {Pt(L–L)} fragment on this carbon is minimal, *i.e* that the platinum is attached at the region of the cage opposite the carbon atom. This is consistent with the known tendency of carbaborane cages to undergo electrophilic substitution at boron atoms opposite carbon. The low-temperature NMR studies[17] of some *exo-nido*-phosphine-rhodacarbaboranes[2] showed that the $[RhL_2]^+$ moiety in these complexes could rotate with respect to, and migrate about, the polyhedral surface of the *nido*-carbaborane cage. Although the results of the NMR experiments are not definitive, they do point to two dynamic processes occurring at room temperature (Scheme 2). One process involves the rotation of the {Pt(L–L)} fragment relative to the cage, leading to the equivalence of the phosphorus environments, whereas the second process requires the {Pt(L–L)} fragment to perambulate about the 12-vertex of the icosahedron so that it is bound in turn to each of the five boron atoms in positions 7–11.

A single-crystal X-ray diffraction study of compound **3c** confirmed the bonding mode of the monocarbaborane cage attached to platinum. The structure (Fig. 1) shows that the complex consists of the $[Pt\{Bu^t_2P(CH_2)_2PBu^t_2\}]^{2+}$ fragment bonded to the carbaborane cage *via* two *exo*-polyhedral three-centre two-electron (Pt ··· H ··· B) bridges.

Structures of complexes involving polyhedral boranes in the chelating mode $\overline{\text{M–H–B–B–H}}$ have been determined

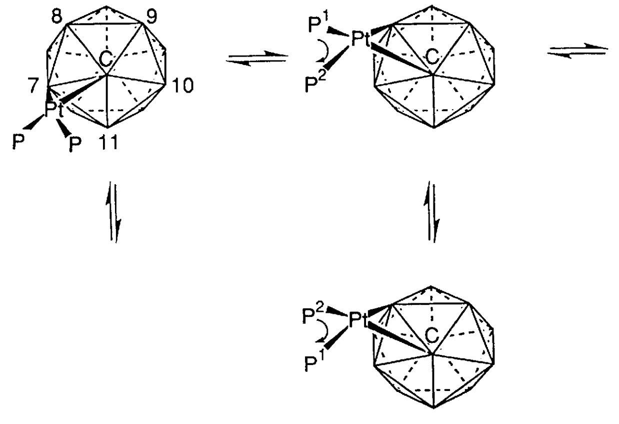

Scheme 2

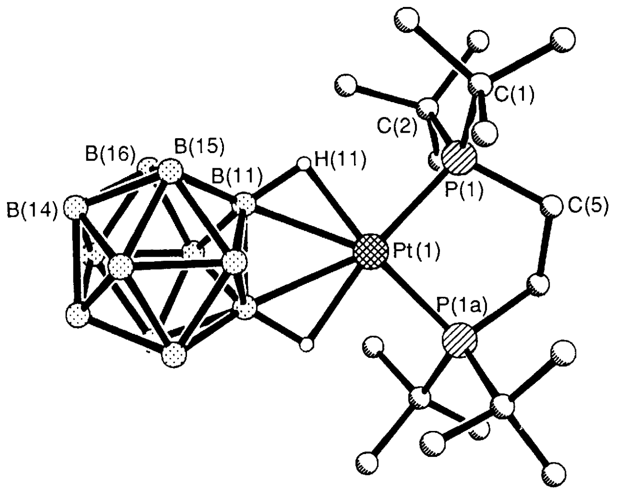

Fig. 1 The molecular structure of cation $[\mathrm{Pt\{Bu^t{}_2P(CH_2)_2PBu^t{}_2\}}(\textit{closo}\text{-}\mathrm{CB_{11}H_{12}})]^+$ **3c** showing the atom numbering scheme. Hydrogen atoms, with the exception of bridging hydrides, have been omitted for clarity

Table 3 Atomic coordinates (× 10^4) for $[\mathrm{Pt\{Bu^t{}_2P(CH_2)_2PBu^t{}_2\}}(\textit{closo}\text{-}\mathrm{CB_{11}H_{12}})][\mathrm{CB_{11}H_{12}}]$ **3c**

Atom	*x*	*y*	*z*
Pt	0	645(1)	2500
P(1)	−980(1)	1612(1)	2459(1)
C(1)	−1703(4)	1487(5)	3378(5)
C(11)	−2141(5)	2270(6)	3592(6)
C(12)	−1199(5)	1221(6)	4245(5)
C(13)	−2363(5)	808(6)	3135(6)
C(2)	−1544(4)	1655(5)	1318(5)
C(21)	−961(5)	2017(6)	664(5)
C(22)	−1821(5)	814(5)	989(6)
C(23)	−2294(5)	2228(6)	1334(6)
C(5)	−436(5)	2578(4)	2666(6)
B(11)	−532(5)	−670(5)	2481(6)
B(12)	6(5)	−996(5)	3481(6)
B(13)	16(6)	−2056(5)	3443(6)
B(14)	−540(6)	−2343(6)	2469(7)
B(15)	−884(6)	−1515(6)	3038(6)
B(16)	−911(6)	−1513(6)	1848(6)
B(21)	−432(8)	−5212(7)	3970(8)
B(22)	−1006(7)	−5205(7)	4926(8)
B(23)	360(7)	−4528(6)	4151(8)
B(24)	−613(6)	−4294(6)	4512(8)
B(25)	604(8)	−5521(7)	4345(9)
B(26)	−267(7)	−5964(6)	4810(7)

Table 4 Selected bond lengths (Å) for $[\mathrm{Pt\{Bu^t{}_2P(CH_2)_2PBu^t{}_2\}}(\textit{closo}\text{-}\mathrm{CB_{11}H_{12}})][\mathrm{CB_{11}H_{12}}]$ **3c** with standard deviations in parentheses

Pt–P(1)	2.253(2)	Pt–B(11)	2.342(8)
Pt–P(1A)	2.253(2)	Pt–B(11A)	2.342(8)
P(1)–C(1)	1.869(8)	P(1)–C(2)	1.879(7)
P(1)–C(5)	1.843(7)	C(1)–C(11)	1.522(13)
C(1)–C(12)	1.548(11)	C(1)–C(13)	1.578(12)
C(2)–C(21)	1.523(11)	C(2)–C(22)	1.534(11)
C(2)–C(23)	1.543(11)	C(5)–C(5A)	1.526(15)
B(11)–B(12)	1.763(12)	B(11)–B(15)	1.741(13)
B(11)–B(16)	1.772(12)	B(11)–B(11A)	1.723(15)
B(11)–B(12A)	1.796(12)	B(12)–B(13)	1.756(13)
B(12)–B(15)	1.770(13)	B(12)–B(11A)	1.796(12)
B(12)–B(16A)	1.792(13)	B(13)–B(14)	1.725(13)
B(13)–B(15)	1.783(14)	B(13)–B(14A)	1.714(14)
B(13)–B(16A)	1.782(14)	B(14)–B(15)	1.722(14)
B(14)–B(16)	1.742(13)	B(14)–B(13A)	1.714(14)
B(14)–B(14A)	1.746(20)	B(15)–B(16)	1.770(13)
B(16)–B(12A)	1.792(13)	B(16)–B(13A)	1.782(14)
B(21)–B(22)	1.749(18)	B(21)–B(23)	1.720(16)
B(21)–B(24)	1.755(16)	B(21)–B(25)	1.810(17)
B(21)–B(26)	1.774(16)	B(22)–B(24)	1.764(16)
B(22)–B(26)	1.753(15)	B(22)–B(23A)	1.732(16)
B(22)–B(25A)	1.720(17)	B(23)–B(24)	1.741(16)
B(23)–B(25)	1.713(15)	B(23)–B(22A)	1.732(16)
B(23)–B(26A)	1.765(16)	B(24)–B(25A)	1.729(18)
B(24)–B(26A)	1.748(15)	B(25)–B(26)	1.770(17)
B(25)–B(22A)	1.720(17)	B(25)–B(24A)	1.729(18)
B(26)–B(23A)	1.765(16)	B(26)–B(24A)	1.748(15)

Table 5 Selected bond angles (°) for $[\mathrm{Pt\{Bu^t{}_2P(CH_2)_2PBu^t{}_2\}}(\textit{closo}\text{-}\mathrm{CB_{11}H_{12}})][\mathrm{CB_{11}H_{12}}]$ **3c** with standard deviations in parentheses

P(1)–Pt–B(11)	113.7(2)	P(1)–Pt–P(1A)	89.4(1)
B(11)–Pt–P(1A)	156.9(2)	P(1)–Pt–B(11A)	156.9(2)
B(11)–Pt–B(11A)	43.2(4)	P(1A)–Pt–B(11A)	113.7(2)
Pt–P(1)–C(1)	112.0(3)	Pt–P(1)–C(2)	110.7(3)
C(1)–P(1)–C(2)	112.0(3)	Pt–P(1)–C(5)	106.5(2)
C(1)–P(1)–C(5)	106.8(4)	C(2)–P(1)–C(5)	108.5(4)
P(1)–C(1)–C(11)	112.4(6)	P(1)–C(1)–C(12)	108.7(5)
C(11)–C(1)–C(12)	107.3(7)	P(1)–C(1)–C(13)	110.9(6)
C(11)–C(1)–C(13)	109.8(6)	C(12)–C(1)–C(13)	107.6(7)
P(1)–C(2)–C(21)	107.9(5)	P(1)–C(2)–C(22)	111.7(5)
C(21)–C(2)–C(22)	109.5(7)	P(1)–C(2)–C(23)	110.4(5)
C(21)–C(2)–C(23)	106.7(7)	C(22)–C(2)–C(23)	110.5(6)
P(1)–C(5)–C(5A)	112.9(4)	Pt–B(11)–B(12)	96.4(4)
Pt–B(11)–B(15)	150.8(6)	B(12)–B(11)–B(15)	60.7(5)
Pt–B(11)–B(16)	148.6(6)	B(12)–B(11)–B(16)	110.1(6)
B(15)–B(11)–B(16)	60.5(5)		

previously.[20–22] With exception of $[\mathrm{Cr(CO)_4(B_2H_4{\cdot}2PMe_3)}]$[22] these have involved d^{10} metal centres and the co-ordination geometry has been quasi-tetrahedral. This mode of bonding for *closo*-boranes is rare and has been structurally characterized only in $[\mathrm{Cu_2B_{10}H_{10}}]$[23] and $[\{\mathrm{Cu(PPh_3)_2}\}_2\mathrm{B_{10}H_{10}}]{\cdot}\mathrm{CHCl_3}$.[24] Not many cases of *exo*-polyhedral (M ··· H ··· B) bonding in transition-metal complexes involving carbaborane ligands have been reported. The complex $[\mathrm{Rh(PPh_3)_2(C_2B_{10}H_{10}Ph)}]$ in which the rhodium centre interacts with the dicarba-*closo*-dodecaborane cage through a Rh–C σ bond and a Rh ··· H ··· B bridge has been described by Allerga *et al.*,[25] and some bidentate *exo-nido*-carbaborane transition-metal complexes have been investigated.[2,16,17] Complex **3c** is the first structurally characterized example of a *closo*-monocarbaborane acting as a bidentate ligand and also the first example of a d^8 ion interacting with a *closo*-polyborane in this manner. The geometry around the Pt atom can be described as distorted square planar with angles [P(1)–Pt–P(1A) 89.4(1)], [H(11)–Pt–H(11A) 106.0(5)], [P(1)–Pt–H(11A) 171.7(2)°] and the dihedral angle defined by planes P(1)–Pt–P(1A) and H(11)–Pt–H(11A) being 0.7°. The Pt–H(11) distance of [1.90(8) Å] lies at the top end of the range (1.656–2.049 Å) reported for Pt–μ-H interactions and is longer than the mean value of (1.610 Å) found for Pt–H (terminal) bonds.[26] The Pt–B distance of [2.342(8) Å] is longer than that observed in compounds involving direct Pt–B interactions, [*closo*-1,1-$(Et_3P)_2$-2,3-Me_2-1,2,3-$PtC_2B_4H_4$] [2.12(1) Å],[27] [$PtCl_2(B_6H_{10})_2$] [2.27(2) Å],[28] and [*nido*-μ-{*trans*-$PtH(Et_3P)_2$}-μ-H-2,3-$C_2B_4H_6$] [2.30(1) Å],[29] as might be expected. The B(11)–Pt–B(11A) angle of [43.2(4)°] is close to the values of 41.7(4) and 42.4(4)° found in [$\{Cu(PPh_3)_2\}_2B_{10}H_{10}$]·$CHCl_3$ where the copper atoms are bound to the *closo*-$B_{10}H_{10}$ ion by $\overline{\text{Cu–H–B–B–H}}$ chelate rings. The Pt–H(11)–B(11) angle of 94(4)° is similar to those found in the $B_{10}H_{10}^{2-}$ complex [85(4)–101(5)°].

The disorder in both carbaborane ions led to difficulty in positioning accurately the carbon atoms. However consideration of the distribution of the B–B bond lengths indicates that, for the anion co-ordinated to the Pt atom, B(14)/B(14A) are the sites for the disordered carbon atom. The B(14)–B distances range from 1.71(1) to 1.75(2) Å (C–B_{cage} 1.716 Å)[30] whereas all the other cage atoms have at least one B–B distance greater than 1.76(1) Å (B–B_{cage} 1.775 Å).[30] This assignment supports the model of platinum-carbaborane co-ordination as the carbon atom is opposite the polyhedron edge interacting with Pt as would be expected,[15] and in addition agrees well with the observation that no Pt–C coupling could be observed in the ^{13}C-{^1H} NMR spectra of complexes **3a**–**3d**.

The disorder and substantially higher thermal parameters associated with the non-co-ordinated anion are reflected in the greater range of B–B distances [1.71(1)–1.81(1) Å] and B–H distances (1.06–1.42 Å). Thus it is more difficult to assign carbon atom positions with confidence. However the atom with the greatest number of short B–B contacts is B(23) and so together with B(23A) provides the probable sites for the disordered carbon atom. The parameters associated with the Pt(dbpe) moiety are similar to those observed previously, Pt–P [2.253(2) Å] in **3c** and 2.262(3), 2.265(3) Å in [$PtCl_2$(dbpe)].[31] The Pt–C(5)–C(5A)–P(1A) system is puckered as observed in co-ordinated ethylenediamine rings with C(5) and C(5A) lying (0.2685 Å) either side of the plane defined by P(1)–P(1A)–Pt.

The conventional non-co-ordinating anions (BF_4^-, ClO_4^-, SbF_6^-, PF_6^-, BPh_4^-, *etc.*) are generally considered to be chemically inert. However in some circumstances, *i.e.* in the presence of a highly co-ordinatively unsaturated metal centre, they have proved reactive enough to become co-ordinated.[32] The monocarba-*closo*-dodecaborane(12) anion $CB_{11}H_{12}^-$ has been suggested[8] to be the least co-ordinating among the so-called non-co-ordinating anions in use at the present time. This was supported by the observation of a uniquely short Ag–C distance for the unidentate benzene ring co-ordinated to silver in [$Ag(C_6H_6)(CB_{11}H_{12})$]·$C_6H_6$.[33] Our work shows that this anion, depending on the nature of the solvent, may co-ordinate producing novel *exo*-diphosphineplatinum-*closo*-monocarbaborane complexes.

The formation of the *exo*-diphosphineplatinum-*closo*-monocarbaborane complexes from the protonation reactions is interesting. It appears likely that the first formed species are the [PtR(L–L)]$^+$ (R = Me or CH_2Bu^t) cations, which are extremely reactive and instead of being stabilized through an α- or γ-agostic interaction they rapidly react with the *closo*-monocarbaborane anion. However the complex so formed, which would be the neutral [$PtR(CB_{11}H_{12})$(L–L)] rapidly undergoes a second protonation–alkane elimination reaction to afford the *exo*-diphosphineplatinum-*closo*-monocarbaborane complexes. Our recent work[5] has shown that protonation of the complexes [$PtEt_2$(L–L)] (L–L = dbpp or dbpx) with the monocarbaborane acid leads to the formation of the cations [PtEt(L–L)]$^+$ which exhibit a β-C–H agostic interaction. Presumably, in the latter case the β-CH bond of the ethyl group competes effectively with the cage for the vacant co-ordination site on the metal, and double protonation does not occur.

Reactions of the exo-*Diphosphineplatinum*-closo-*monocarbaborane Complexes with Donor Ligands*.—The co-ordinated carbaborane cage in the *exo*-diphosphineplatinum-*closo*-monocarbaborane complexes is readily displaced by hard σ-donating ligands. Thus complexes **3b**–**3d** react with acetonitrile within 1 h to yield the acetonitrile complexes [$Pt(NCMe)_2$(L–L)][$CB_{11}H_{12}$]$_2$ (L–L = dbpp **6b**; dbpe, **6c**; dbpx, **6d**) (Scheme 1). The ^{31}P-{^1H} NMR spectra of **6b**–**6d** (Table 1) each show a single signal with platinum-195 satellites. Likewise **3b** reacts with pyridine to afford the pyridine complex [$Pt(NC_5H_5)_2$(dbpp)][$CB_{11}H_{12}$]$_2$ **7** for which the ^{31}P-{^1H} NMR spectrum also shows a single peak with platinum-195 satellites. The ^1J(PtP) values for **6b**–**6d** and **7** (Table 1) are typical for complexes in which nitrogen is bonded to platinum.[34,35] This displacement was also confirmed by (*i*) the disappearance of the co-ordinated carbaborane cage signal in the ^{13}C-{^1H} NMR spectrum of **6b** and (*ii*) the disappearance of the Pt···H···B bridge resonance in the ^1H NMR spectrum of **6d**. It is interesting that the *exo*-diphosphineplatinum-*closo*-monocarbaborane complexes are not affected by C_2H_4, CO, or PPh_3. Thus no reaction was observed when **3b** or **3d** was stirred in an atmosphere of C_2H_4 or CO, and the *exo*-diphosphineplatinum-*closo*-monocarbaborane complexes were recovered unchanged. Likewise **3b** was recovered unchanged when an acetone solution of it and PPh_3 (2 molar equivalents) was heated at 50 °C in a sealed tube under nitrogen for 15 h. The reactions of some *exo*-*nido*-phosphinerhodacarbaboranes with various phosphines, CO, and dihydrogen have been reported.[17] The reaction of the thf complex **5** with deuteriated acetonitrile affords [$PtMe(NCCD_3)$(dbpp)][$CB_{11}H_{12}$] **8** for which spectroscopic data (Tables 1 and 2) are typical for similar complexes.[34]

Experimental

All the solvents were dried prior to use by distillation under nitrogen over sodium–benzophenone or CaH_2, unless stated otherwise. All operations were carried out on a vacuum/nitrogen line in conventional Schlenk-type vessels unless stated otherwise. The NMR solvents were degassed by the freeze–thaw method. Microanalyses were performed by Butterworth Laboratories, Middlesex. The IR spectra were recorded on a Perkin-Elmer 1710 FTIR instrument as Nujol mulls, NMR on a Bruker AC 300 (300.13, ^1H; 121.49, ^{31}P; 75.45, ^{13}C; and 96.2 MHz, ^{11}B) spectrometer. The diphosphines 1,3-bis(dicyclohexylphosphino)propane (dcpp),[36] 1,3-bis(di-*tert*-butylphosphino)propane (dbpp),[37] 1,2-bis(di-*tert*-butylphosphino)ethane (dbpe),[38] and 1,2-bis(di-*tert*-butylphosphinomethyl)benzene (dbpx),[39] the acid $HCB_{11}H_{12}$[15] and the complexes [$PtMe_2$(cod)],[11] [$Pt(CH_2Bu^t)_2$(cod)],[12] and *cis*-[$PtCl_2(NCBu^t)_2$][39] were prepared by published methods. The preparation of [$PtCl_2$(dbpe)] has already been described.[31] The complex [$PtCl_2$(dbpx)] was prepared by a modification of the reported method.[39] The analytical and spectroscopic data for the new complexes are given in Tables 1 and 2.

Syntheses.—[$PtCl_2$(dbpx)]. A solution of dbpx (0.422 g, 1.07 mmol) and *cis*-[$PtCl_2(NCBu^t)_2$] (0.462 g, 1.07 mmol) in degassed 2-methoxyethanol (10 cm^3) was heated at 70 °C in a sealed tube under nitrogen for 20 h. A pale yellow crystalline solid was formed and more of the solid crystallized on cooling (–20 °C). The solvent was removed by a syringe and the pale yellow product [$PtCl_2$(dbpx)] dried *in vacuo* (0.26 g).

Dimethyl complexes. (*a*) [$PtMe_2$(dcpp)] **1a**. To a solution of dcpp (0.155 g, 0.355 mmol) in toluene (5 cm^3) was added a solution of [$PtMe_2$(cod)] (0.118 g, 0.355 mmol) in toluene (10 cm^3). A white crystalline solid was immediately formed, and the reaction mixture was stirred for 0.5 h to allow the reaction to go to completion. The mixture was then filtered and the product washed with hexane (3 × 5 cm^3) and dried *in vacuo* affording white microcrystals of [$PtMe_2$(dcpp)] **1a** (0.185 g).

(*b*) [$PtMe_2$(dbpp)] **1b**. To a solution of dbpp (0.162 g, 0.487

mmol) in toluene (1.5 cm^3) was added [$PtMe_2$(cod)] (0.162 g, 0.487 mmol). The resulting solution was heated at 80 °C in a sealed tube under nitrogen for 12 h. The solution was allowed to cool to room temperature and subsequent cooling to −20 °C afforded white crystals of [$PtMe_2$(dbpp)] **1b** (0.18 g).

(*c*) [$PtMe_2$(dbpe)] **1c** and [$PtMe_2$(dbpx)] **1d**. To a stirred suspension of [$PtCl_2$(L–L)] (L–L = dbpe or dbpx, typically 0.3 g) in diethyl ether (15 cm^3) at 0 °C was added LiMe (slightly in excess of 2 molar equivalents). After 2 h the excess of LiMe was hydrolysed using an ice-cold saturated aqueous solution of ammonium chloride. The ether layer was decanted and the aqueous layer extracted with ether (3 × 10 cm^3). The ether fractions were dried over $MgSO_4$. Filtration and evaporation of the ether *in vacuo* afforded [$PtMe_2$(dbpe)] **1c** or [$PtMe_2$(dbpx)] **1d**.

Dineopentyl complexes. (*a*) [$Pt(CH_2Bu^t)_2$(dcpp)] **2a**. To a stirred solution of dcpp (0.401 g, 0.918 mmol) in diethyl ether (20 cm^3) was added [$Pt\{CH_2Bu^t\}_2$(cod)] (0.409 g, 0.918 mmol). After 48 h the solvent was removed *in vacuo* and the residue crystallized from hexane at −20 °C affording white crystals of [$Pt\{CH_2Bu^t\}_2$(dcpp)] **2a** (0.43 g).

(*b*) [$Pt(CH_2Bu^t)_2$(L–L)] (L–L = dbpp, **2b**; *or* dbpe, **2c**). A solution of dbpp or dbpe (typically 0.4 g) and [$Pt(CH_2Bu^t)_2$(cod)] (1 mol equivalent) in CH_2Cl_2 (15 cm^3) was heated at 65 °C in a sealed tube under nitrogen for 2 h. The solvent was then removed *in vacuo* and the residue crystallized from CH_2Cl_2–toluene or -hexane at −20 °C affording white crystals of [$Pt(CH_2Bu^t)_2$(L–L)].

Protonations.—[PtR_2(dcpp)] (R = Me, **1a**; *or* CH_2Bu^t, **2a**). To a stirred solution of complex **1a** or **2a** (typically 0.15 g) in diethyl ether (10 cm^3) at 0 °C was added $HCB_{11}H_{12}$ (1 mol equivalent). After *ca.* 1 h an off-white precipitate was formed. The reaction mixture was allowed to warm to room temperature and the precipitate allowed to settle. The supernatant was then filtered and discarded, and the product washed with ether (3 × 5 cm^3). Crystallization from chloroform–diethyl ether afforded off-white microcrystals of [Pt(dcpp)(*closo*-$CB_{11}H_{12}$)][$CB_{11}H_{12}$] **3a**. A similar reaction in a 1:2 mol ratio also afforded **3a**.

[PtR_2(L–L)] (R = Me, L–L = dbpp, **1b**; *or* dbpe, **1c**; R = CH_2Bu^t, L–L = dbpp, **2b**; *or* dbpe, **2c**). To a stirred solution of **1b**, **2b**, **1c** or **2c** (typically 0.15 g) in diethyl ether (10 cm^3) at 0 °C was added $HCB_{11}H_{12}$ (1 mol equivalent). After *ca.* 1 h the reaction mixture was allowed to warm to room temperature and then filtered. Evaporation of the filtrate *in vacuo* afforded residues which were washed with ether (3 × 5 cm^3). Crystallization from dichloromethane–diethyl ether afforded pale yellow crystals of [Pt(L–L)(*closo*-$CB_{11}H_{12}$)][$CB_{11}H_{12}$] (L–L = dbpp, **3b**; or dbpe, **3c**). The reaction mixture for complex **1c** after filtration gave a residue which was crystallized in dichloromethane–diethyl ether and the spectroscopic data and elemental analysis (Tables 1 and 2) for this material showed that the complex may be formulated as [PtMe($CB_{11}H_{12}$)(dbpe)] **4**. A similar reaction in a 1:2 mol ratio also afforded **3b** or **3c**.

[$PtMe_2$(dbpx)] **1d**. To a stirred solution of complex **1d** (0.044 g, 0.071 mmol) in diethyl ether (10 cm^3) at 0 °C was added $HCB_{11}H_{12}$ (0.58 cm^3, 0.142 mmol). After *ca.* 1 h the reaction mixture was allowed to warm to room temperature and then filtered. Evaporation of the filtrate *in vacuo* gave a residue which was crystallized from acetone–diethyl ether (vapour diffusion) affording pale yellow crystals of [Pt(dbpx)(*closo*-$CB_{11}H_{12}$)][$CB_{11}H_{12}$] **3d** (0.059 g).

[$PtMe_2$(dbpp)] **1b** *in thf.* To a stirred solution of complex **1b** (0.083 g, 0.149 mmol) in thf (10 cm^3) at 0 °C was added $HCB_{11}H_{12}$ (1.1 cm^3, 0.149 mmol). After 0.5 h the solution was allowed to warm to room temperature, the solvent removed *in vacuo*, and the residue washed with ether (2 × 5 cm^3). Crystallization from thf–ether at −20 °C afforded [PtMe(thf)(dbpp)][$CB_{11}H_{12}$] **5** (0.072 g) as a diethyl ether solvate.

Reaction of [Pt(L–L)(*closo*-$CB_{11}H_{12}$)][$CB_{11}H_{12}$] (L–L = dbpp, **3b**; dbpe, **3c**; *or* dbpx, **3d**) *with Acetonitrile*.—Complexes **3b**–**3d** (typically 0.030 g) were treated with either deuteriated or normal acetonitrile (0.5 cm^3) and their ^1H, $^{13}C-\{^1H\}$, and $^{31}P-\{^1H\}$ NMR spectra recorded after about 1 h. Crystallization from acetonitrile–diethyl ether (vapour diffusion) afforded the products [$Pt(NCMe)_2$(L–L)][$CB_{11}H_{12}$]$_2$ (L–L = dbpp, **6b**; dbpe, **6c**; *or* dbpx, **6d**).

Reaction of [Pt(dbpp)(*closo*-$CB_{11}H_{12}$)][$CB_{11}H_{12}$] **3b** *with Pyridine*.—Complex **3b** (0.030 g, 0.037 mmol) was treated with pyridine (0.5 cm^3) and the resulting solution left to stand for 1 h. Crystallization from pyridine–hexane (vapour diffusion) afforded white crystals of [$Pt(NC_5H_5)_2$(dbpp)][$CB_{11}H_{12}$]$_2$ **7** (0.025 g).

Reaction of [PtMe(thf)(dbpp)][$CB_{11}H_{12}$] **5** *with Acetonitrile*.—Complex **5** (0.040 g, 0.053 mmol) was treated with deuteriated acetonitrile (0.5 cm^3) and its ^1H, $^{13}C-\{^1H\}$, and $^{31}P-\{^1H\}$ NMR spectra recorded after about 1 h indicated the formation of [PtMe($NCCD_3$)(dbpp)][$CB_{11}H_{12}$] **8**.

Crystal Structure Determination and Refinement of Complex **3c**.—*Crystal data*. $C_{20}H_{64}B_{22}P_2Pt$, $M = 799.6$, monoclinic, space group $C2/c$, $a = 16.199(4)$, $b = 16.564(5)$, $c = 14.896(3)$ Å, $\beta = 93.64(2)°$, $U = 3989(2)$ Å^3, $Z = 4$, $D_c = 1.331$ g cm^{-3}, $F(000) = 1608$, μ(Mo-Kα) = 36.48 cm^{-1}, crystal size *ca.* 0.3 × 0.2 × 0.1 mm, $\lambda = 0.710\ 37$ Å.

Data collection. Diffraction measurements were made on a Nicolet R3m/V four-circle diffractometer at 213 K using graphite-monochromated Mo-Kα radiation and θ–2θ scans. A total of 4513 reflections was collected ($3 < 2\theta < 50°$), the index range being $0 \leqslant h \leqslant 19$, $-2 \leqslant k \leqslant 19$, $-17 \leqslant l \leqslant 17$. There were 3400 unique reflections ($R_{int} = 0.03$) of which 2842 satisfied the criterion $F > 4\sigma(F)$ and were used in refinement. The intensities were corrected for absorption using an azimuthal scan technique, maximum and minimum transmission factors 0.93 and 0.50. Complex neutral scattering factors were obtained from ref. 40.

Structure solution and refinement. The structure was solved by direct methods and refined in space group $C2/c$ by full-matrix least-squares routines the quantity minimized being $w(F_o - F_c)^2$. The choice of space group was based on the following observations: (*a*) the refinement proceeded more smoothly in $C2/c$ than in Cc; (*b*) the bond length range for chemically equivalent bonds was considerably smaller in the centrosymmetric space group (*e.g.* the C–C distances in the Bu^t groups ranged from 1.522(13) to 1.578(12) Å in $C2/c$ and from 1.404 to 1.792 Å in Cc), (*c*) the estimated standard deviations (e.s.d.s) in Cc were twice the size of those calculated in $C2/c$. However refinement in $C2/c$ imposes crystallographic two-fold symmetry on the cation and the anion centroid is at a crystallographic inversion centre. Consequently the carbaborane groups are disordered in this model and refinement proceeded by assigning boron scattering factors to all cage atoms.

All non-hydrogen atoms were allowed to refine anisotropically. All hydrogen atoms associated with the carbaborane were located from ΔF maps and those in the Bu^t groups were placed in calculated positions. The hydrogen atoms were given fixed isotropic thermal parameters and allowed to ride on the appropriate boron or carbon atoms except for the positional parameters of the μ-hydrogen which were successfully refined. At convergence $R = 0.043$ and $R' = 0.050$ where $w^{-1} = \sigma^2(F_o) + 0.0011F_o^2$; the corresponding residuals for all data were $R = 0.057$ and $R' = 0.056$. An empirical extinction correction was applied $\chi = 0.000\ 13$. The goodness-of-fit was 1.00, the largest $\Delta/\sigma < 0.001$ and the data-to-parameter ratio 13.7:1. The final difference map revealed peaks of 1.27 and 0.89 e Å^{-3} at distances of 1.35 ad 1.01 Å from the Pt atom. All the remaining peaks were <0.76 e Å^{-3}, map minimum −0.71 e Å^{-3}.

All calculations were performed using the SHELXTL-PLUS[41] program suite on a MicroVAX II computer. Table 3 lists the fractional atomic coordinates, 4 and 5 the bond lengths and angles respectively. Fig. 1 shows the numbering scheme used.

Additional material available from the Cambridge Crystallographic Data Centre comprises H-atom coordinates, thermal parameters and remaining bond lengths and angles.

Acknowledgements

We thank Dr. S. J. Simpson for obtaining low temperature $^{31}P-\{^1H\}$ and $^{11}B-\{^1H\}$ NMR spectra. We also thank NORAD/University of Dar-es-Salaam and the SERC for studentships (to G. S. M. and S. A. L. respectively).

References

1 (*a*) H. M. Colquhoun, T. J. Greenhough and M. G. H. Wallbridge, *J. Chem. Soc., Chem. Commun.*, 1980, 192; (*b*) M. Green, J. A. K. Howard, A. P. James, A. N. de M. Jelfs, C. M. Nunn and F. G. A. Stone, *J. Chem. Soc., Dalton Trans.*, 1987, 81.
2 C. B. Knobler, T. B. Marder, E. A. Misuzawa, R. G. Teller, J. A. Long, P. E. Behnken and M. F. Hawthorne, *J. Am. Chem. Soc.*, 1984, **106**, 2990.
3 C. J. Jones, J. N. Francis and M. F. Hawthorne, *J. Am. Chem. Soc.*, 1973, **95**, 7633.
4 N. Carr, B. J. Dunne, A. G. Orpen and J. L. Spencer, *J. Chem. Soc., Chem. Commun.*, 1988, 926.
5 L. Mole, N. Carr, A. G. Orpen and J. L. Spencer, *Organometallics*, 1991, **10**, 49.
6 Z. Dawoodi, M. L. H. Green, V. S. B. Mtetwa, K. Prout, A. J. Schultz, A. J. Williams and T. F. Koetzle, *J. Chem. Soc., Dalton Trans.*, 1986, 1629.
7 W. H. Knoth, *Inorg. Chem.*, 1971, **10** 598.
8 K. Shelly, C. A. Reed, Y. J. Lee and W. R. Scheidt, *J. Am. Chem. Soc.*, 1986, **108**, 3117.
9 G. P. Gupta, G. Lang, Y. J. Lee, W. R. Scheidt, K. Shelly and C. A. Reed, *Inorg. Chem.*, 1987, **26**, 3022.
10 G. S. Mhinzi and J. L. Spencer, unpublished work.
11 H. C. Clark and L. E. Manzer, *J. Organomet. Chem.*, 1973, **59**, 411.
12 P. Foley, R. DiCosimo and G. M. Whitesides, *J. Am. Chem. Soc.*, 1980, **102**, 6713.
13 P. S. Pregosin and R. W. Kunz, ^{31}P *and* ^{13}C *NMR of Transition Metal Phosphine Complexes*, Springer, New York, 1979, p. 16.
14 R. H. Reamey and G. M. Whitesides, *J. Am. Chem. Soc.*, 1984, **106**, 81.
15 T. Jelinek, J. Plesek, S. Hermanek and B. Stibr, *Collect Czech. Chem. Commun.*, 1986, **51**, 819.
16 J. A. Doi, R. G. Teller and M. F. Hawthorne, *J. Chem. Soc., Chem. Commun.*, 1980, 80.
17 J. A. Long, T. B. Marder, P. E. Behnken and M. F. Hawthorne, *J. Am. Chem. Soc.*, 1984, **106**, 2979.
18 H. Beall and H. C. Bushweller, *Chem. Rev.*, 1973, 465.
19 J. Plesek, T. Jelinek, E. Drdakova, S. Hermanek and B. Stibr, *Collect. Czech. Chem. Commun.*, 1984, **49**, 1559.
20 S. A. Snow, M. Shimoi, C. D. Ostler, B. K. Thompson, G. Kodama and R. W. Parry, *Inorg. Chem.*, 1984, **23**, 512.
21 M. Shimoi, K. Katoh, H. Tobita and H. Ogino, *Inorg. Chem.*, 1990, **29**, 814.
22 M. Shimoi, K. Katoh and H. Ogino, *J. Chem. Soc., Chem. Commun.*, 1990, 811.
23 R. B. Dobrott and W. N. Lipscomb, *J. Chem. Phys.*, 1962, **37**, 1779.
24 J. T. Gill and S. J. Lippard, *Inorg. Chem.*, 1975, **14**, 751.
25 C. Allerga, M. Calligaris, R. Furlanetta, G. Nardin and L. Randaccio, *Cryst. Struct. Commun.*, 1974, **3**, 69.
26 A. G. Orpen, L. Brammer, F. H. Allen, O. Kennard, D. G. Watson and R. Taylor, *J. Chem. Soc., Dalton Trans.*, 1989, S1.
27 G. K. Barker, M. Green, F. G. A. Stone and A. J. Welch, *J. Chem. Soc., Dalton Trans.*, 1980, 1186.
28 J. P. Brennan, R. Schaeffer, A. Davison and S. S. Wreford, *J. Chem. Soc., Chem. Commun.*, 1973, 354.
29 G. K. Barker, M. Green, F. G. A. Stone, A. J. Welch, T. P. Onak and G. Siwapanyoyos, *J. Chem. Soc., Dalton Trans.*, 1979, 1687.
30 F. H. Allen, O. Kennard, D. G. Watson, L. Brammer, A. G. Orpen and R. Taylor, *J. Chem. Soc., Perkin Trans. 2*, 1987, S1.
31 M. Harada, Y. Kai, N. Yasuoka and N. Kasai, *Bull. Chem. Soc. Jpn.*, 1976, **49**, 3472.
32 E. Horn and M. R. Snow, *Aust. J. Chem.*, 1984, **37**, 1375 and refs. therein.
33 K. Shelly, D. C. Finster, Y. J. Lee, W. R. Scheidt and C. A. Reed, *J. Am. Chem. Soc.*, 1985, **107**, 5955.
34 T. G. Appleton and M. A. Bennett, *Inorg. Chem.*, 1978, **17**, 738.
35 G. Mingetti, G. Banditelli and F. Bonati, *J. Chem. Soc., Dalton Trans.*, 1979, 1851.
36 K. Issleb and A. Tzschach, *Chem. Ber.*, 1959, **92**, 1118.
37 L. Mole, Ph.D. Thesis, University of Salford, 1990.
38 A. A. del Paggio, R. A. Andersen and E. L. Muetterties, *Organometallics*, 1987, **6**, 1260.
39 C. J. Moulton, Ph.D. Thesis, University of Leeds, 1976.
40 *International Tables for X-Ray Crystallography*, Kynoch Press, Birmingham, 1974, vol. 4.
41 G. M. Sheldrick, SHELXTL-PLUS Release 3–4 for Nicolet R3m/V Crystallographic Research Systems, University of Gottingen, 1988.

Received 30*th April* 1991; *Paper* 1/02040D